ORIGINAL PAPER

Neumann–Neumann–Schur complement methods for Fekete spectral elements

**Richard Pasquetti · Francesca Rapetti ·
Luca Pavarino · Elena Zampieri**

Abstract   For the iterative solution of the Schur complement system associated with the discretization of an elliptic problem by means of a triangular spectral element method (TSEM), Neumann–Neumann (NN) type preconditioners are constructed and studied. The TSEM approximation, based on Fekete nodes, is a generalization to non-tensorial elements of the classical Gauss–Lobatto–Legendre quadrilateral spectral elements. Numerical experiments show that the TSEM Schur complement condition number grows linearly with the polynomial approximation degree, N, and quadratically with the inverse of the mesh size, h. NN preconditioners for the Schur complement allow to reduce the N-dependence of the condition number, by solving local Neumann problems on each spectral element, and to eliminate the h-dependence if an additional coarse solver is employed. Numerical results indicate that, in spite of the more severe ill-conditioning, the condition number of the TSEM preconditioned operator satisfies the same bound as that of the standard SEM, i.e., $Ch^{-2}(1 + \log N)^2$ for one-level NN preconditioning and $C(1 + \log N)^2$ for two-level Balancing Neumann-Neumann (BNN) preconditioning.

R. Pasquetti (✉) · F. Rapetti
Laboratoire J.-A. Dieudonné, CNRS & Université de Nice et Sophia-Antipolis, Parc Valrose,
06108 Nice cedex 02, France
e-mail: richard.pasquetti@unice.fr

F. Rapetti
e-mail: francesca.rapetti@unice.fr

L. F. Pavarino · E. Zampieri
Department of Mathematics, Universitá di Milano, Via Saldini 50, 20133 Milano, Italy
e-mail: Luca.Pavarino@mat.unimi.it

E. Zampieri
e-mail: Elena.Zampieri@mat.unimi.it

1 Introduction

When complex geometries are involved, the implementation of high-order methods is a challenging task. To date, the most successful approaches are the so-called *hp*-finite-element methods and spectral element methods (e.g., [1–3]). Both are based on polynomial approximations of high degree; The former uses a modal approach, whereas the latter uses a nodal approach. In standard spectral-element methods (SEM), the set of nodes are provided by the tensorial product of one-dimensional Gauss–Lobatto–Legendre (GLL) points.

The development of spectral-element formulations for complex geometries naturally leads to unstructured meshes. Accordingly, spectral-element methods based on triangular/tetrahedral elements (TSEM) have been introduced [4–7] and applied to large-scale simulations, as, e.g., in [8]. However, because the choice of nodes is less straightforward for triangles than for quadrangles (2D case), different possibilities have been investigated (e.g., [9–11]). In this work, we consider the Fekete points [12, 13] as in our previous work [14–16].

Once an accurate and suitable TSEM approximation has been provided, efficient solvers for the resulting algebraic system must be developed. This task is quite challenging for high-order discretizations, especially in our case, since the TSEM algebraic system is more ill-conditioned than its standard element counterpart. Despite efforts made to fine-tune the approximation points, the condition number deteriorates rapidly when increasing the polynomial approximation degree, N. Previously, we discussed the use of overlapping Schwarz preconditioners, with each spectral element being considered as a subdomain [16]. In the 2D (3D) case, one spectral element may indeed contain more than 100 (1000) nodes. Our numerical results show that Schwarz preconditioners with generous overlap, defined by all adjacent spectral elements, are optimal, i.e., the condition number of the preconditioned operator is bounded by a constant independent of both N and element size, h. While in the SEM case it is possible to construct Schwarz preconditioners with small overlap by extending each element (subdomain) with a few rows of GLL nodes of the neighboring elements [17–20], a similar technique can not be designed straightforwardly for the TSEM case since the element Fekete points are not distributed as a tensor product.

In this paper, we consider instead algorithms that belong to the family of non-overlapping domain-decomposition methods, more precisely the so-called Neumann–Neumann (NN) family; see [21 Chap. 6] for a general introduction and [22, 23] for the SEM case. As previously, we consider each spectral element as a different subdomain and setup the Schur complement system for the boundary nodes of the triangles. The one-level NN preconditioner allows us to achieve a convergence rate that is nearly independent of the polynomial approximation degree N and the two-level Balancing Neumann–Neumann (BNN) preconditioner, which additionally employs a coarse solver (balancing stands here for coarse grid solving), further eliminates the dependence on the number of spectral elements, yielding a scalable preconditioner. This approach does not suffer from high computational cost due to the forced generous overlap of the TSEM Schwarz preconditioner, and therefore presents a computational cost comparable to that of BNN for standard SEM. Our results indicate that the condition number of the TSEM preconditioned operator satisfies the same bound as that of the standard SEM, i.e., $Ch^{-2}(1 + \log N)^2$ for one-level NN preconditioning and $C(1 + \log N)^2$ for two-level BNN preconditioning.

We center our discussion on the model elliptic Helmholtz problem:

$$
\begin{aligned}
-\nu \Delta u + u &= f &&\text{in } \Omega, \\
u &= 0 &&\text{on } \partial\Omega,
\end{aligned}
\tag{1}
$$

where ν is a positive coefficient, Ω the computational domain and $\partial\Omega$ its boundary. Note that the inhomogeneous Dirichlet case can immediately be recovered by a suitable lifting. For simplicity, we only consider the 2D case, though the techniques presented in this paper apply equally well to more general 3D elliptic problems. This model equation must be solved at each time step when implicit time discretizations of the unsteady diffusion or Navier–Stokes equations are considered. In Sect. 2, we recall some basics of the

TSEM and make some remarks on its implementation (see [15] for details). In Sect. 3, we introduce the NN and BNN Schur complement methods for TSEM approximations. In Sect. 4, we provide numerical examples to check the efficiency of these methods. Finally, we present some conclusions in Sect. 5.

2 The Fekete–Gauss spectral element method

The weak formulation of problem (1) reads: Given $f \in L^2(\Omega)$, find $u \in E = H_0^1(\Omega)$ (standard notations are used for these spaces, see e.g., [24]) such that

$$a(u,v) := \int_\Omega (\nu \, \nabla u \cdot \nabla v + u \, v) \, \mathrm{d}\mathbf{x} = \int_\Omega f \, v \, \mathrm{d}\mathbf{x} \quad \forall v \in E. \tag{2}$$

The variational formulation (2) is discretized by a conforming SEM based on triangles. This Galerkin method employs a discrete space consisting of continuous piecewise polynomials of degree N (e.g., [2] for a general introduction). Let $T = \{(r,s): -1 \le r, s, r+s \le 0\}$ be the reference triangle and $\mathcal{P}_N(T)$ the set of polynomials on T of total degree $\le N$. We assume that Ω is decomposed into K non-overlapping triangular finite elements Ω_k, $\overline{\Omega} = \bigcup_{k=1}^K \overline{\Omega}_k$, each of which is the image of T by means of a suitable mapping, i.e., $\Omega_k = \boldsymbol{g}_k(T)$. The intersection between two distinct Ω_k is either the empty set or a common vertex or a common side. For the approximation space, say $E_{K,N}$, we use continuous, piecewise polynomials of total degree $\le N$,

$$E_{K,N} = \{v \in E : v|_{\Omega_k} \circ \boldsymbol{g}_k \in \mathcal{P}_N(T), \, 1 \le k \le K\}. \tag{3}$$

Let $n = (N+1)(N+2)/2$ and $\{\psi_j\}_{j=1}^n$ be an orthonormal basis of $\mathcal{P}_N(T)$ for the usual $L^2(T)$ inner product (for example, the Koornwinder–Dubiner polynomials may be used to constitute such a basis [25]). The Fekete points on T are defined as the points $\{\hat{\mathbf{x}}_i\}_{i=1}^n$ that maximize the determinant of the Vandermonde matrix V with elements $V_{ij} = \psi_j(\hat{\mathbf{x}}_i)$, $1 \le i, j \le n$. Among the main properties of Fekete points proved in [12, 13, 26], one has that, on the sides of the triangle, the Fekete and GLL points coincide and that Fekete points are GLL points for the cube, thus providing a strong link with the usual SEM.

Unlikely GLL points, a quadrature formula based on Fekete points is only exact for integrands in $\mathcal{P}_N(T)$. This observation suggests to separate the sets of approximation and quadrature points, using the Fekete points $\{\hat{\mathbf{x}}_i\}_{i=1}^n$ for the first set and other points $\{\hat{\mathbf{y}}_i\}_{i=1}^m$ for the second set, defined by imposing an exact integration of polynomials, e.g., in $\mathcal{P}_{2N}(T)$; see [15]. Given the values at the approximation points of a polynomial $u_N \in \mathcal{P}_N(T)$, one can setup interpolation and differentiation matrices to compute the values of u_N and its derivatives, respectively, at the quadrature points. The interpolation matrix is simply $V'V^{-1}$, where V' is a matrix of dimension (m,n) such that $V'_{ij} = \psi_j(\hat{\mathbf{y}}_i)$. To compute derivatives, e.g., with respect to r, at the quadrature points we use again the Koornwinder–Dubiner polynomials to obtain $D^r = V'^r V^{-1}$, with $(V'^r)_{ij} = \partial_r \psi_j(\hat{\mathbf{y}}_i)$. Once such differentiation matrices are known, D^r and D^s, it is an easy task to compute derivatives at the quadrature points starting from the values at the approximation points by applying the chain rule.

Our TSEM approach makes use of highly accurate integration rules based on Gauss points [27–29]. If such integration rules are unknown, e.g., for large values of N, it is possible, but at a higher computational cost, to use integration rules based on Gauss points for the quadrangle and then map them to T (e.g., [2, 30]). On a generic triangle $\Omega_k = \boldsymbol{g}_k(T)$:

$$(u,v)_{\Omega_k,N} = \sum_{j=1}^m u(\boldsymbol{g}_k(\hat{\mathbf{y}}_j)) \, v(\boldsymbol{g}_k(\hat{\mathbf{y}}_j)) \, |J_k(\hat{\mathbf{y}}_j)| \, \omega_j, \tag{4}$$

where $\omega_j > 0, 1 \le j \le m$, are the quadrature weights and $|J_k|$ the Jacobian of the mapping $\boldsymbol{g}_k$ between T and Ω_k. Knowing how to compute derivatives and integrals, we can use the usual finite-element methodology

to set the discrete problem

$$\sum_{k=1}^{k=K} a_{k,N}(u,v) = \sum_{k=1}^{k=K} (f,v)_{k,N} \quad \forall v \in E_{K,N}, \tag{5}$$

where $a_{k,N}(\cdot,\cdot)$ is obtained from $a(\cdot,\cdot)$ by replacing each integral with the quadrature rule (4). Equation 5 can be written in matrix form as a linear system $A\mathbf{u} = \mathbf{b}$. Note that the TSEM matrix A is less sparse than the standard SEM matrix and more ill-conditioned. As for some related choices of the basis functions, its condition number is expected to grow as $O(N^4 h^{-2})$, where h is a characteristic diameter of the triangular spectral elements (e.g., [31, 32]).

3 Neumann–Neumann methods for Fekete spectral elements

There are several approaches to the numerical solution of the linear system $A\mathbf{u} = \mathbf{b}$. Besides direct methods, which can be very expensive and far from being optimal for large-scale problems, common approaches are based on the iterative solution by a preconditioned Krylov subspace method such as the preconditioned conjugate gradient (PCG) for symmetric and positive-definite matrices A. Among all possible preconditioning techniques, we consider methods that use non-overlapping subdomains, namely, Schur complement or substructuring methods [21, 33]. The specificity here is that each spectral element is assimilated to a subdomain. The basic idea is to setup an equation for the boundary nodes of the spectral elements, solve the resulting algebraic system with a PCG method and finally compute independently the solution at the interior nodes of each spectral element.

Let us denote by Γ the skeleton of the domain decomposition, i.e., the set of interfaces of the spectral elements $\Gamma = \cup \overline{\partial \Omega}_k \setminus \overline{\partial \Omega}$, and use (i) the subscript I for the block of unknowns associated with the Fekete nodes in the interior and on the true exterior boundary of any substructure and (ii) the subscript Γ for the block of unknowns associated with the interior boundary of a substructure facing one or more neighboring substructures. By reordering the interior nodes and then the exterior ones, we can rewrite the matrix system $A\mathbf{u} = \mathbf{b}$ as

$$\begin{pmatrix} A_{II} & A_{I\Gamma} \\ A_{\Gamma I} & A_{\Gamma\Gamma} \end{pmatrix} \begin{pmatrix} \mathbf{u}_I \\ \mathbf{u}_\Gamma \end{pmatrix} = \begin{pmatrix} \mathbf{b}_I \\ \mathbf{b}_\Gamma \end{pmatrix}. \tag{6}$$

Assuming now that A_{II} is not singular, we can eliminate the variables $\mathbf{u}_I$ associated with the interior of the substructures, and setup the following equation for $\mathbf{u}_\Gamma$:

$$S\mathbf{u}_\Gamma = \mathbf{g} \quad \text{with} \tag{7}$$

$$S = (A_{\Gamma\Gamma} - A_{\Gamma I} A_{II}^{-1} A_{I\Gamma}), \tag{8}$$

$$\mathbf{g} = \mathbf{b}_\Gamma - A_{\Gamma I} A_{II}^{-1} \mathbf{b}_I. \tag{9}$$

The so-called Schur complement matrix S is of smaller dimension than matrix A, being of dimension (n_Γ, n_Γ) where n_Γ is the number of nodes on Γ, and moreover is better conditioned. This is because:

$$\mathbf{x}^T A \mathbf{x} = \mathbf{x}_\Gamma^T S \mathbf{x}_\Gamma \quad \text{if} \tag{10}$$

$$A_{II} \mathbf{x}_I + A_{I\Gamma} \mathbf{x}_\Gamma = 0, \tag{11}$$

so that the maximum (minimum) eigenvalue of A, equal to the maximum (minimum) of the Rayleigh quotient $\mathbf{x}^T A \mathbf{x}/\mathbf{x}^T \mathbf{x}$, is certainly greater (smaller) than the maximum (minimum) eigenvalue of S [33]. In the framework of domain decomposition methods and $\mathcal{P}_1$ finite elements the following theorem can be shown [21],

Theorem 1 *The condition number of the Schur operator is bounded by*

$$\kappa(S) \leq \frac{C}{hH}, \tag{12}$$

where H and h are the diameters of subdomains and finite elements, respectively.

If each spectral element is regarded as a subdomain, one has $\kappa(S) \leq C(N)/h^2$. Knowing that on each edge the Fekete nodes coincide with the GLL nodes, the behavior of $C(N)$ is in fact assessed in [32]. In this paper, it is proved that, for both the triangle and the quadrangle, if the basis functions are Lagrangian polynomials and if the side and vertex basis functions are based on the GLL points, then $C(N) \sim N$. Consequently one can state:

Theorem 2 *For a Fekete spectral element approximation of problem* (1)*, the condition number of the Schur operator is bounded by*

$$\kappa(S) \leq \frac{CN}{h^2}, \tag{13}$$

where C is a constant, h the diameter of the finite element and N the degree of the polynomial approximation.

Let us note that by setting $h = H/N$ in (12), which is an average mesh size of the Fekete (or GLL) "micromesh", and then using the usual notation h for the spectral element diameter, we recover the bound (13).

  Similarly to matrix A and vector $\mathbf{b}$, S and $\mathbf{g}$ may be setup by assembling the local contributions, i.e., by the so-called stiffness summation technique. If we denote by $\sum'$ this operation, we thus have:

$$S = \sum_k{}' S_k, \quad S_k = (A_{\Gamma\Gamma,k} - A_{\Gamma I,k} A_{II,k}^{-1} A_{I\Gamma,k}), \tag{14}$$

$$\mathbf{g} = \sum_k{}' \mathbf{g}_k, \quad \mathbf{g}_k = \mathbf{b}_{\Gamma,k} - A_{\Gamma I,k} A_{II,k}^{-1} \mathbf{b}_{I,k}, \tag{15}$$

where $A_k, k = 1, K$, denotes the contribution of the spectral element k to A. It remains to provide efficient preconditioners for the Schur complement matrix S.

3.1 A one-level NN preconditioner

Suppose that Ω is a square simply divided into two triangles. Then, by symmetry, $S_1 = S_2$ and the stiff summation resumes to the usual sum, $S = S_1 + S_2 = 2S_1$. In this case, S_1 is clearly a perfect preconditioner to S. From this naive observation, one can deduce the Dirichlet–Neumann preconditioner as well as the NN preconditioner and these standard denominations indeed trace back to the two subdomains case. The NN preconditioner is especially well adapted when many subdomains are involved. This involves using the preconditioner:

$$F_{\mathrm{NN}} = \sum_k{}' D_k S_k^{-1} D_k, \tag{16}$$

where D_k is a diagonal matrix such that D_k^{-1} gives the number of spectral elements shared by the Fekete boundary nodes (2, for an edge node, 3 or more for a vertex node). Better convergence is obtained when using such weighting matrices. Of course:

$$\sum_k{}' D_k = I, \tag{17}$$

where I is the identity matrix.

  Let us recall that the local Schur complements and their inverses are generally not setup:

– The action of the Schur complement S_k is mediated by three matrix-vector multiplications and one matrix solve, corresponding to solving a Dirichlet problem in Ω_k; see (14).

– The action of S_k^{-1} is mediated by solving a Neumann problem. Indeed, one can show that (see [33] for details):

$$A_k^{-1} = \begin{pmatrix} \cdots & \cdots \\ \cdots & S_k^{-1} \end{pmatrix}, \tag{18}$$

so that the action of S_k^{-1} on a vector $\mathbf{v}_{\Gamma,k}$ can be computed like:

$$S_k^{-1}\mathbf{v}_{\Gamma,k} = (0\ I)A_k^{-1} \begin{pmatrix} 0 \\ \mathbf{v}_{\Gamma,k} \end{pmatrix}. \tag{19}$$

In the framework of our approach, i.e., each Fekete spectral element constitutes a subdomain, it is also possible to setup the local Schur complements and their inverses. But despite the increasing storage capacity of modern computers, this remains unrealistic in 3D.

For $\mathcal{P}_1$ finite elements, one has the following upper bound for the condition number of the matrix $F_{\text{NN}}S$ [21]:

Theorem 3 *The condition number of the Neumann–Neumann operator is bounded by*

$$\kappa(F_{\text{NN}}S) \leq C\,\frac{1}{H^2}\left(1 + \log\frac{H}{h}\right)^q, \tag{20}$$

where H and h are the diameters of subdomains and finite elements, respectively, with $q = 2$ for finite element meshes with cross points and when using the weighting matrices D_k.

For Fekete spectral elements, one may then expect:

$$\kappa(F_{\text{NN}}S) \leq C\frac{1}{h^2}(1 + \log N)^2 \tag{21}$$

and this result in fact holds for standard GLL quadrilateral spectral elements [22].

The h^{-2} dependence of the condition number is typical of finite-element iterative solvers that do not use a coarse solver. The NN algorithm is thus not scalable and this may be very penalizing when H is minimum, as it is when each spectral element is considered as a subdomain. The inclusion of a coarse-grid problem reduces this dependence on the number of subdomains significantly. This is the reason for introducing a balancing NN algorithm in the next section.

3.2 A two-level BNN preconditioner

To avoid the $O(1/h^2)$ scaling of κ, a coarse solver is recommended. The BNN method is simply the one-level NN preconditioner with the addition of a particularly simple coarse grid correction. The BNN algorithm makes use of the coarsest one, since only one unknown is associated with each spectral element, i.e., the correction is constructed by using a piecewise constant coarse grid space. Moreover, the coarse correction operator, say A_0, is very simple to build, as it results from a simple aggregation of the Schur complement, S.

To this end, we introduce the restriction matrix R_0 of dimension (K, n_Γ), where n_Γ is the number of nodes at the spectral-element interfaces: $[R_0]_{ij}^{-1}$ gives the number of elements shared by the node j of the element i. With $\mathbf{v}$ denoting a vector of boundary-node values, $R_0\mathbf{v}$ is a vector of element values that provides local weighted sums of $\mathbf{v}$. The extension operator is simply obtained by transposition. The aggregated matrix A_0 then reads

$$A_0 = R_0 S R_0^T. \tag{22}$$

Note that such a matrix is generally singular. This is obvious if Ω only shows two subdomains: because R_0 has two identical lines, their sum weighted with $(1, -1)$ is the null vector. This idea may easily be extended

to a regular mesh of rectangles, as the one used in Sect. 4, by using the opposite weights $(1, -1)$ to all pairs of triangles that share an edge. In such cases, R_0 is not of maximum rank and consequently A_0 is singular. However, for a mesh composed of 3 triangles sharing a vertex, with the boundary Fekete points for $N = 3$, i.e., the vertices and the middle of each edge, then one can check that R_0 is of rank 3. To eliminate the possible singularity of A_0, one may use a pseudo-inverse. Another possibility is to remove one subdomain, i.e., one spectral element, and setup a matrix A_0 of dimension $(K - 1, K - 1)$.

Since the Schur complement is not setup in practice, it may appear problematic to build A_0. However, with obvious notations,

$$A_0 = \sum_{k=1}^{K} A_{0k}, \quad A_{0k} = R_{0k} S_k R_{0k}^T \tag{23}$$

which means that each $(S_k)_{ij}$ must be equidistributed between the $(A_{0k})_{lm}$ such that the node i (local index in element k) belongs to the element l, and the node j belongs to the element m.

Once the matrix A_0 has been setup, one can use the following symmetric preconditioner, directly inspired from [34]:

$$F_{\text{BNN}} = F_0 + (I - F_0 A) F_{\text{NN}} (I - A F_0), \tag{24}$$

where $F_0 = R_0^T A_0^{-1} R_0$. Applying such a preconditioner yields the three steps algorithm:

$$\mathbf{u}^* = \mathbf{u}^n + F_0 (\mathbf{b} - A \mathbf{u}^n), \tag{25}$$

$$\mathbf{u}^{**} = \mathbf{u}^* + F_{\text{NN}} (\mathbf{b} - A \mathbf{u}^*), \tag{26}$$

$$\mathbf{u}^{n+1} = \mathbf{u}^{**} + F_0 (\mathbf{b} - A \mathbf{u}^{**}), \tag{27}$$

where $\mathbf{u}^n$ is the value of $\mathbf{u}$ at iteration n [33].

For $\mathcal{P}_1$ finite elements, one can prove the following upper bound for the condition number of the matrix $F_{\text{BNN}} S$ [21].

Theorem 4 *The condition number of the balancing Neumann–Neumann operator is bounded by*

$$\kappa(F_{\text{BNN}} S) \leq C \left(1 + \log \frac{H}{h} \right)^q, \tag{28}$$

where H and h are the diameters of subdomains and finite elements, respectively, with $q = 2$ for finite element meshes with cross points and using the weighting matrices D_k.

For Fekete spectral elements, one can then expect that

$$\kappa(F_{\text{BNN}} S) \leq C (1 + \log N)^2. \tag{29}$$

4 Numerical experiments

In this section, we report results obtained for the model problem (1) with $\nu = 1$ discretized into Fekete–Gauss spectral elements. We first investigate numerically the N- and h-dependence of the condition number of the system matrix A and of the Schur complement S, without and with the NN or BNN preconditioners. We then carry out convergence tests of the numerical solution for a problem with a known exact solution.

The spectral element mesh is simply obtained by first dividing $\Omega = (-1, 1)^2$ in I^2 rectangles and then by dividing each element into two triangular spectral elements. Thus, $K = 2I^2$ and the grid-size parameter h equals $2/I$. Computations have been carried out for different values of the total polynomial approximation degree, i.e., $N = \{3, 6, 9, 12, 15, 18\}$, and varying the number of spectral elements, $I = \{4, 6, 8, 10\}$ (i.e., $1/h = \{2, 3, 4, 5\}$).

For the convergence tests, the body force f is consistent with $u(x, y) = \sin(\pi x) \sin(\pi y)$ as an exact solution of (1). The resulting Schur complement problem is solved by the conjugate-gradient (CG) method without preconditioning, with the NN preconditioner (16) and with the BNN preconditioner (24). The initial guess is zero and the stopping criterion is $|\mathbf{r}^{(k)}|/|\mathbf{r}^{(0)}| \leq 10^{-8}$, where $\mathbf{r}^{(k)}$ is the kth residual.

Results obtained with a deformed domain are also presented. In this case, the computational domain Ω is deformed into a quadrilateral with vertices $(-1, -1)$, $(1, -1)$, $(0, 1)$, $(-1, 1)$, so that all triangles are different, using the mapping $(x, y) \mapsto ((-xy + 3x - y - 1)/4, y)$. In the convergence tests, the body force f corresponds to the exact solution $u(x, y) = \sin(\pi x) \sin(\pi y) (2x + y - 1)/3$.

4.1 Condition number

The ill-conditioning feature of Fekete spectral-element approximations is illustrated in Fig. 1 (left), where the variation of the condition number $\kappa(A)$ with N is given for different $I = \{4, 6, 8, 10\}$. For $N \geq 12$, one can check that $\kappa(A) \sim N^4$. The same results are given in Fig. 1 (right), in order to demonstrate the dependence of $\kappa(A)$ with respect to h. As expected, we obtain a quadratic increase with respect to $1/h$.

Similar results are given for the Schur complement, S, in Fig. 2. As expected, one finds $\kappa(S) \leq \kappa(A)$ and a quadratic increase with respect to $1/h$. Moreover, it is numerically confirmed that, for Fekete spectral elements $\kappa(S) \sim N$, which is favorable by being similar to the one obtained for the classical SEM.

Results for the NN algorithm are reported in Fig. 3. As discussed in Sect. 3, we always have a quadratic variation of $\kappa(F_{NN} S)$ with $1/h$. We do not have a power law for the N-dependence and rather expect that, similarly to the standard SEM, $\kappa(F_{NN} S) \sim h^{-2}(1 + \log N)^2$. To demonstrate this dependence, in Fig. 3 (left) we plot $\kappa^{0.5}(F_{NN} S)$ with respect to N in a semi-log plot. One may indeed observe that, for $N \geq 6$, the
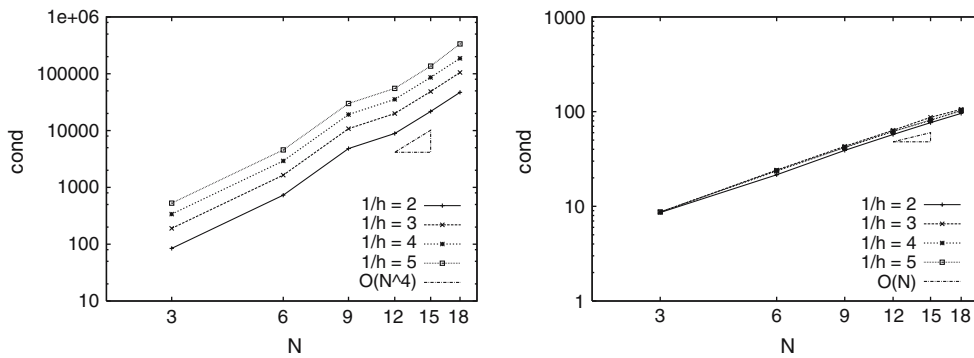

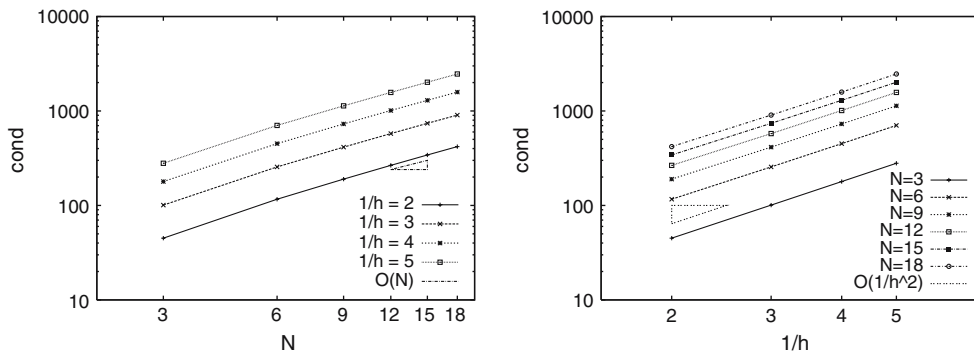**Fig. 1** N- and h-dependence of the condition number of the Fekete system matrix A

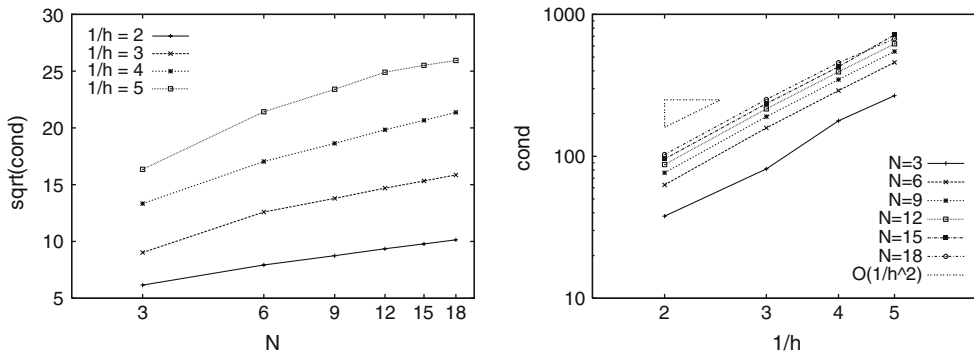**Fig. 2** N- and h-dependence of the condition number of the Fekete–Schur complement S

Fig. 3 N- and h-dependence of the condition number of the NN-preconditioned Schur complement, $F_{NN}S$
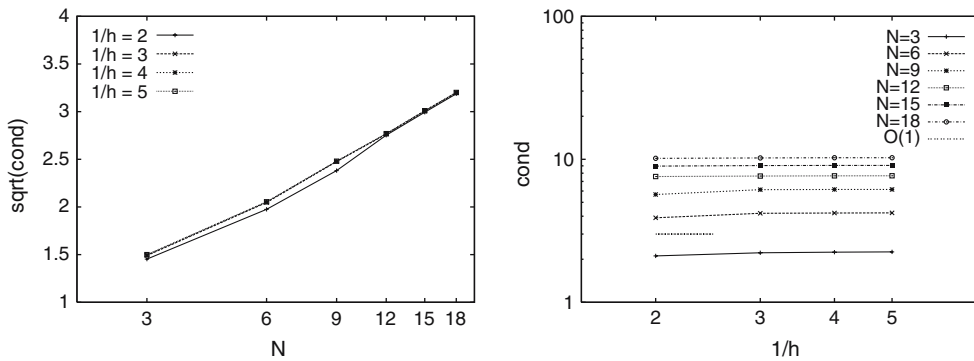

Fig. 4 N- and h-dependence of the condition number of the BNN-preconditioned Schur complement, $F_{BNN}S$

variation of $\kappa^{0.5}(F_{NN}S)$ with respect to $\log N$ is close to linear, so that one may conjecture that the GLL spectral-elements behavior remains with Fekete spectral elements. However, note that, even though the NN preconditioning has a beneficial influence, especially for the larger N, the condition numbers obtained with and without NN preconditioning are of the same magnitude.

Finally, results obtained with the balancing NN algorithm are shown in Fig. 4, revealing a strong influence on the condition number, which, as expected, becomes independent of h and only weakly dependent on N. Here again we observe that the variations of $\kappa^{0.5}(F_{BNN}S)$ with respect to N are close to linear.

Next, we demonstrate the influence of a mesh deformation on the present results. In Fig. 5 we give the variations with respect to N of the condition number of the system matrix A and of the non-preconditioned, NN preconditioned and BNN preconditioned Schur complement matrix S, for the non-deformed and deformed domains and the mesh obtained with $I = 4$.

As expected, mesh deformation causes an increase in the condition number. However, a drastic influence of the deformation is not observed.

4.2 Convergence tests

In Fig. 6, the variations of the error with respect to the number iterations are plotted for the Schur complement without preconditioning and with the NN and BNN preconditioners. Results are given for $N = 18$ and $I = 6$. As expected, a large gain is obtained by using the BNN preconditioner. However, only a small gain when using the NN preconditioner is observed. This is consistent with the condition numbers of S and $F_{NN}S$ being of the same magnitude. In terms of CPU time, using the BNN preconditioner is only justified for large-scale problems, which is not the case here. An efficient implementation is also required.
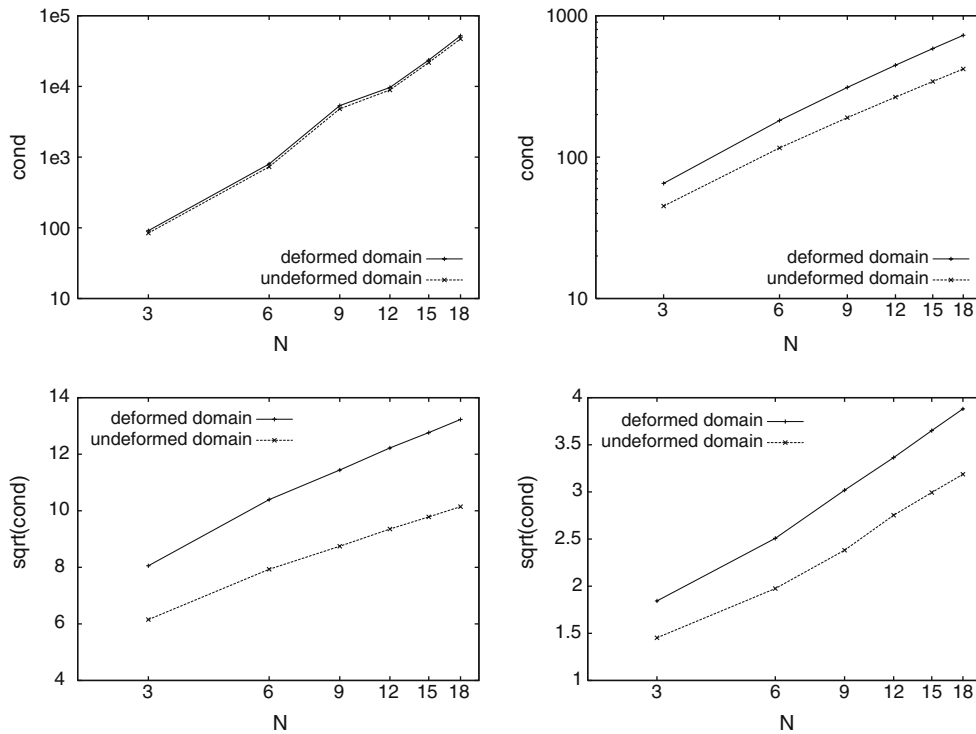
Fig. 5 Deformed domain: N-dependence of the condition number of the matrices A (up left), S (up right), $F_{NN}S$ (down left) and $F_{BNN}S$ (down right)

Table 1 CG solutions for the matrices A and S, $N = 12$ and $I = \{4, 6, 8, 10\}$. Rows 1–4 refer to the case $\Omega = [-1, 1]^2$, whereas rows 5–8 refer to the deformed domain

	A				S			
$1/h$	It.	λ_{max}	λ_{min}	κ	It.	λ_{max}	λ_{min}	κ
2	360	90.69	1.01e−2	8899.93	62	10.76	4.05e−2	265.68
3	516	90.95	4.55e−3	19955.99	86	10.82	1.87e−2	576.12
4	641	91.04	2.56e−3	35439.02	105	10.84	1.07e−2	1011.57
5	755	91.09	1.64e−3	55345.76	123	10.84	6.90e−3	1571.64
2	574	97.56	1.01e−2	9645.53	116	18.81	4.20e−2	446.87
3	864	95.07	4.53e−3	20978.90	177	20.14	1.95e−2	1031.47
4	1151	93.97	2.55e−3	36746.56	243	20.92	1.11e−2	1876.63
5	1440	93.36	1.63e−3	56941.69	313	21.43	7.18e−3	2984.28

Let us now carry out systematic comparisons between the performances of the developed iterative solvers. for the fixed grid with $I = 4$ ($1/h = 2$), we vary the polynomial degree $N = \{3, 6, 9, 12, 15, 18\}$; For the fixed polynomial degree $N = 12$, we vary the grid $I = \{2, 4, 6, 8\}$. The study is carried out for the non-deformed and deformed domains. The conjugate gradient method is used to solve systems based on the matrices A, S, $F_{NN}S$ and $F_{BNN}S$. Results are given in Tables 1–4, where we report the iteration counts (It.), spectral condition number (κ) and extreme eigenvalues (λ_{max}, λ_{min}).

Results obtained for $N = 3$ are not particularly significant, as in this case there is only one interior Fekete node. For $N \geq 6$, it appears efficient to use the complement system, because, as previously mentioned, $\kappa(S) \sim N$. Using the one-level NN preconditioner allows to decrease the condition number without real

Table 2 CG solutions for the matrices $F_{NN}S$ and $F_{BNN}S$, $N = 12$ and $I = \{4, 6, 8, 10\}$. Rows 1–4 refer to the case $\Omega = [-1, 1]^2$, whereas rows 5–8 refer to the deformed domain

	$F_{NN}S$				$F_{BNN}S$			
$1/h$	It.	λ_{max}	λ_{min}	κ	It.	λ_{max}	λ_{min}	κ
2	38	87.51	1.0044	87.12	18	7.04	1.0011	7.03
3	84	217.43	1.0066	215.98	25	7.64	1.0	7.64
4	129	396.63	1.0082	393.37	26	7.66	1.0	7.66
5	169	625.87	1.0090	620.25	26	7.68	1.0	7.68
2	68	150.25	1.0061	149.34	31	11.33	1.0	11.33
3	131	418.73	1.0081	415.35	34	12.55	1.0	12.55
4	206	834.33	1.0101	825.98	35	13.39	1.0	13.39
5	284	1406.97	1.0116	1390.82	36	13.99	1.0	13.99

Table 3 CG solutions for A and S, $I = 4$ and $N = \{3, 6, 9, 12, 15, 18\}$. Rows 1–6 refer to the case $\Omega = [-1, 1]^2$, whereas rows 7–12 refer to the deformed domain

	A				S			
N	It.	λ_{max}	λ_{min}	κ	It.	λ_{max}	λ_{min}	κ
3	33	13.77	0.16	84.34	24	9.25	0.20	45.04
6	103	29.76	4.08e−2	729.56	41	10.20	8.77e−2	116.26
9	251	87.25	1.81e−2	4820.56	50	10.54	5.55e−2	190.03
12	360	90.69	1.01e−2	8899.93	62	10.76	4.05e−2	265.68
15	550	141.76	6.52e−3	21739.58	70	10.91	3.18e−2	342.41
18	850	212.76	4.52e−3	47043.80	78	11.03	2.62e−2	419.88
3	57	14.77	0.16	91.15	46	13.93	0.21	65.23
6	167	32.36	4.04e−2	799.11	76	16.55	9.12e−2	181.50
9	411	96.15	1.79e−2	5351.92	96	17.94	5.76e−2	311.20
12	574	97.56	1.01e−2	9645.53	116	18.81	4.20e−2	446.87
15	875	152.56	6.47e−3	23568.96	132	19.40	3.31e−2	585.78
18	1348	233.78	4.48e−3	52075.53	148	19.83	2.72e−2	726.74

Table 4 CG solutions for $F_{NN}S$ and $F_{BNN}S$, with $I = 4$ and $N = \{3, 6, 9, 12, 15, 18\}$

	$F_{NN}S$				$F_{BNN}S$			
N	It.	λ_{max}	λ_{min}	κ	It.	λ_{max}	λ_{min}	κ
3	20	37.85	1.0058	37.63	10	2.11	1.0	2.11
6	31	62.90	1.0044	62.62	14	3.90	1.0	3.90
9	36	76.49	1.0036	76.22	16	5.67	1.0013	5.67
12	38	87.51	1.0044	87.12	18	7.04	1.0011	7.03
15	44	95.72	1.0038	95.35	20	8.97	1.0011	8.96
18	45	102.92	1.0042	102.49	21	10.17	1.0015	10.16
3	40	65.87	1.0150	64.89	15	3.40	1.0	3.40
6	52	108.88	1.0074	108.08	23	6.29	1.0	6.29
9	62	131.68	1.0061	130.87	28	9.11	1.0	9.11
12	68	150.25	1.0061	149.34	31	11.33	1.0	11.33
15	73	164.00	1.0064	162.95	33	13.35	1.0011	13.33
18	76	176.07	1.0062	174.98	36	15.07	1.0012	15.06

Rows 1–6 refer to the case $\Omega = [-1, 1]^2$, whereas rows 7–12 refer to the deformed domain

Fig. 6 Convergence history for the CG method with S (CG), $F_{NN}S$ (PNNCG) and $F_{BNN}S$ (PBNNCG), for $N = 18$ and $I = 6$
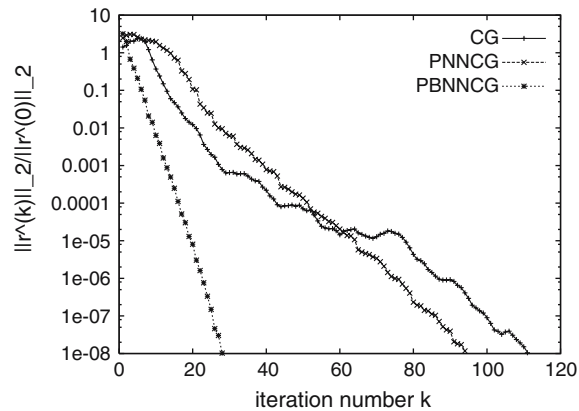
improvements on the the convergence rate. Impressive results are only obtained for the BNN preconditioner. In fact, it seems that for the solution strategy presented in this paper, i.e., each Fekete spectral element is assimilated to a subdomain, the efficiency of the preconditioner is essentially pivoted on the use of a coarse solver. This point will be addressed in future work.

5 Conclusion

It is well known that solving efficiently the algebraic systems resulting from a high-order spectral approximation is generally more challenging than solving for low-order discretizations. In this paper, we have applied non-overlapping domain decomposition techniques to the Schur complement system arising from the Fekete–Gauss spectral-element approximation (TSEM). Considering each spectral element as a subdomain, we have derived the Schur complement system acting on the grid point values of the triangle boundaries, studied its conditioning properties and constructed efficient Neumann–Neumann preconditioners. The original TSEM system matrix is more ill-conditioned than the standard SEM system matrix, with a condition number that scales as N^4 versus N^3. Nevertheless, the condition number of the TSEM Schur complement was observed to still scale as N, just as in the standard SEM. In order to further improve the conditioning of the discrete system, we focused on NN preconditioners for the Schur complement that weaken the N-dependence of the condition number by solving local Neumann problems on each spectral element and eliminate the h-dependence if an additional coarse solver is employed. Our results indicate that, in spite of the original more severe ill-conditioning, the condition number of the TSEM preconditioned operator satisfies the same bound as in the case of standard SEM, i.e., $Ch^{-2}(1+\log N)^2$ for one-level NN preconditioning and $C(1+\log N)^2$ for two-level BNN preconditioning. In terms of convergence rates, the best results have been obtained with the BNN preconditioner.

References

1. Schwab C (1998) p- and hp-Finite Element Methods. Theory and Applications in Solid and Fluid Mechanics. Oxford University Press, New York p 374
2. Karniadakis GE, Sherwin SJ (1999) Spectral hp Element Methods for CFD. Oxford Univ. Press, London p 390
3. Deville MO, Fischer PF, Mund EH (2002) High-order methods for incompressible fluid flow. Cambridge University Press, p 499
4. Taylor MA, Wingate BA (1998) A generalized diagonal mass matrix spectral element method for non-quadrilateral elements. Appl Num Math 33:259–265
5. Hesthaven JS, Teng CH (2000) Stable spectral methods on tetrahedral elements. SIAM J Sci Comput 21:2352–2380
6. Warburton TA, Pavarino LF, Hesthaven JS (2000) A pseudo-spectral scheme for the incompressible Navier-Stokes equations using unstructured nodal elements. J Comput Phys 164:1–21

7. Hesthaven JS, Warburton T (2002) Nodal high-order methods on unstructured grids. J Comp Phys 181:186–221
8. Giraldo FX, Warburton T (2005) A nodal triangle-based spectral element method for the shallow water equations on the sphere. J Comp Phys 207:129–150
9. Chen Q, Babuvska I (1995) Approximate optimal points for polynomial interpolation of real functions in an interval and in a triangle. Comput Methods Appl Mech Engg 128:485–494
10. Chen Q, Babuvska I (1996) The optimal symmetrical points for polynomial interpolation of real functions in a tetrahedron. Comput Methods Appl Mech Engg. 137:89–94
11. Hesthaven JS (1998) From electrostatic to almost optimal nodal sets for polynomial interpolation in a simplex. SIAM J Numer Anal 35:655–676
12. Taylor MA, Wingate BA, Vincent RE (2000) An algorithm for computing Fekete points in the triangle. SIAM J Numer Anal 38:1707–1720
13. Bos L, Taylor MA, Wingate BA (2001) Tensor product Gauss–Lobatto points are Fekete points for the cube. Math Comput 70:1543–1547
14. Pasquetti R, Rapetti F (2004) Spectral element methods on triangles and quadrilaterals: comparisons and applications. J Comput Phys 198:349–362
15. Pasquetti R, Rapetti F (2006) Spectral element methods on unstructured meshes: comparisons and recent advances. J Sci Comput 27:377–387 (Proc. of the ICOSAHOM 2004 Congress)
16. Pasquetti R, Pavarino LF, Rapetti F, Zampieri E (2006) Overlapping Schwarz preconditioners for Fekete spectral elements. In: Proc. of the 16th int. conf. on domain decomposition methods, Lecture Notes in Computational Science and Engineering
17. Casarin MA (1997) Quasi-optimal Schwarz methods for the conforming spectral element discretization. SIAM J Numer Anal 34:2482–2502
18. Klawonn A, Pavarino LF (1998) Overlapping Schwarz methods for mixed linear elasticity and Stokes problems. Comput Meths Appl Mech Engg 165:233–245
19. Fischer PF (1997) An overlapping Schwarz method for spectral element solution of the incompressible Navier–Stokes equations. J Comput Phys 133:84–101
20. Fischer PF, Lottes JW (2005) Hybrid Schwarz-Multigrid methods for the spectral element method: extensions to Navier–Stokes. J Sci Comput 6:345–390
21. Toselli A, Widlund O (2005) Domain Decomposition Methods – Algorithms and Theory. Springer, Berlin Heidelberg New York, p 450
22. Pavarino LF (1997) Neumann–Neumann algorithms for spectral elements in three dimensions. RAIRO M^2AN 31: 471–493
23. Pavarino LF, Widlund OB (2002) Balancing Neumann–Neumann methods for incompressible Stokes equations. Comm Pure Appl Math 55:302–335
24. Girault V, Raviart P-A (1986) Finite Element Methods for Navier–Stokes equations. Theory and Algorithms. Springer-Verlag, Berlin, p 374
25. Dubiner M (1991) Spectral methods on triangles and other domains. J Sci Comput 6:345–390
26. Bos L (1991) On certain configurations of points in $\mathbb{R}^n$ which are unisolvent for polynomial interpolation. J Approx Theory 64:271–280
27. Stroud AH (1971) Approximate Calculations of Multiple Integrals. Prentice-Hall, p 431
28. Cools R (2002) Advances in multidimensional integration. J Comput Appl Math 149:1–12
29. Demkowicz L, Walsh T, Gerdes K, Bajer A (1998) 2D hp-adaptative finite element package Fortran 90 implementation (2Dhp90). TICAM Report 98–14
30. Stroud AH, Secrest D (1966) Gaussian Quadrature Formulas. Prentice-Hall, p 374
31. Hu NH, Guo XZ, Katz IN (1998) Bounds for eigenvalues and condition numbers in the p-version of the finite element method. Math Comput 67:1423–1450
32. Melenk JM (2002) On condition numbers in hp-FEM with Gauss-Lobatto based shape functions. J Comput Appl Math 139:21–48
33. Smith BF, Bjorstad PE, Gropp WD (1996) Domain Decomposition: Parallel Multilevel Methods for Elliptic Partial Differential Equations. Cambridge University Press p 224
34. Mandel J, Brezina M (1996) Balancing domain decomposition for problems with large jumps in coefficients. Math Comp 65:1387–1401